

# Transport of helium in polycarbonate membranes<sup>☆</sup>

Mar López-González<sup>a</sup>, Enrique Saiz<sup>b,\*</sup>, Evaristo Riande<sup>a</sup>, Julio Guzmán<sup>a</sup>

<sup>a</sup>Instituto de Ciencia y Tecnología de Polímeros (CSIC), 28006 Madrid, Spain

<sup>b</sup>Departamento de Química-Física, Universidad de Alcalá, Alcalá de Henares, 28871 Madrid, Spain

It is a pleasure to dedicate this paper to Prof. Wayne L. Mattice

## Abstract

The transport of helium in membranes of poly(bisphenol A carbonate-co-4,4'-(3,3,5-trimethylcyclohexylidene)diphenyl carbonate) (PBCDC) is reported. The experimental values of the diffusion and permeability coefficients, under the upstream pressure of 176 cmHg, are  $(10.9 \pm 0.7) \times 10^{-6} \text{ cm}^2 \text{ s}^{-1}$  and  $61.4 \pm 0.5$  barrers, respectively, at 30°C. Both coefficients obey Arrhenius behavior with activation energies of 1.9 and 3.0 kcal mol<sup>-1</sup>, respectively. The dynamics of helium in the membranes was simulated using the transition state approach (TSA). Very good agreement between the theoretical and experimental values of the diffusion coefficient was found. However, the simulated solubility coefficient is nearly one order of magnitude higher than the experimental value. © 2001 Elsevier Science Ltd. All rights reserved.

**Keywords:** Transition state approach; Helium; Polycarbonate membranes

## 1. Introduction

There is a growing interest in the study of gas transport in polymers as these substances continue to be the principal raw materials for the preparation of membranes for gas separation. The results on hand suggest that the polymers used for this purpose should have bulky segments in their chemical structures that impede efficient packing of the chains. If these structural characteristics are fulfilled, gas flow greatly increases without severely damaging the permselectivity of the membranes [1–3]. Moreover, bulky segments also enhance the glass transition of the membranes thus diminishing aging effects that may negatively affect gas transport.

Concurrent with the experimental studies in gas transport is the need to understand, at the molecular level, the dramatic changes that some permeation factors may experience by effect of small modifications in the chemical structure of glassy membranes. In principle, molecular dynamics should be a suitable tool for the prediction of gas transport in membranes as a function of their chemical structure. However, the computing time needed to reach the diffusive regime may be prohibitively large, even in the rubbery state.

To overcome this shortcoming of the MD techniques, the so-called transition states approach (TSA) was developed which assumes that small molecules diffuse in polymers by thermally activated jumps [4]. Moreover, in the time scales relevant for gas transport, the TSA assumes that polymer chains fluctuate about certain fixed average positions.

Experimental and simulation studies on the diffusion dynamics of argon in membranes of poly(bisphenol A carbonate-co-4,4'-(3,3,5-trimethylcyclohexylidene)diphenyl carbonate) (PBCDC) were recently carried out [5]. Good agreement between experimental and simulated results was found by assuming that the jump of a diffusant molecule from a site to another adjacent site depends not only on the barrier energy separating both sites, but also on the ratio of the crest surface to the cross-section area of the diffusant. It is a purpose of this paper to check the validity of this latter assumption by performing a comparative study of the experimental and simulated results for the transport of helium in the membranes indicated. A scheme representing the chemical structure of PBCDC membranes is shown in Fig. 1.

## 2. Experimental section

The membranes were prepared at 300°C by compression molding of PBCDC supplied by Aldrich. The time of residence of the membrane in the mold was 15 min and then the membrane was rapidly cooled at room temperature. The glass transition temperature of the membrane was measured

<sup>☆</sup> This paper was originally submitted to *Computational and Theoretical Polymer Science* and received on 2 January 2001; received in revised form on 30 March 2001; accepted on 2 April 2001. Following the incorporation of *Computational and Theoretical Polymer Science* into *Polymer*, this paper was consequently accepted for publication in *Polymer*.

\* Corresponding author. Tel.: +34-91-8854-664; fax: +34-91-8854-763.

E-mail address: enrique.saiz@uah.es (E. Saiz).

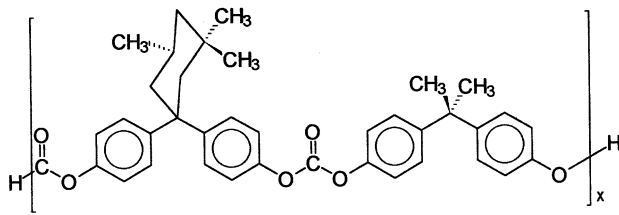


Fig. 1. Schematic representation of PBCDC chains.

with a DSC7 Perkin Elmer calorimeter at a heating rate of  $10^{\circ}\text{C min}^{-1}$ . The value of  $T_g$  taken at the onset of the departure of the endotherm from the base line was  $205^{\circ}\text{C}$ .

Permeation measurements were performed with an experimental device that basically consists of two chambers separated by the membrane. Vacuum was made in the two chambers and helium at a predetermined pressure was suddenly introduced into the upstream chamber. The pressure in this compartment was measured with a Gometric transducer operating in the 0–10 bars interval. The evolution of the pressure in the downstream chamber was measured with a MKS 627B transducer operating in the range  $10^{-4}$ –1 mmHg. All the measurements were performed keeping the permeation cell in thermostatic conditions. As usual, the pressure on the air inlet in the downstream chamber was measured as a function of time just before each experiment, and further subtracted from the curve representing the pressure of helium versus time in this chamber.

### 3. Experimental results

As usual, the curves depicting the variation of the pressure of the downstream chamber with time present a transitory region at short times followed by a straight line at long times reflecting steady-state conditions. An illustrative curve is shown in Fig. 2. The curves are described by the following equation obtained by integrating Fick's second law using appropriate boundary conditions [6].

$$p(t) = 0.2876 \frac{p_0 A l S T}{V} \left[ \left( \frac{Dt}{l^2} - \frac{1}{6} \right) - \frac{2}{\pi^2} \sum_{n=1}^{\infty} \frac{(-1)^n}{n^2} \exp\left(-\frac{n^2 \pi^2 D}{l^2} t\right) \right] \quad (1)$$

where  $T$  is the absolute temperature,  $p_0$  (in cmHg) and  $V$  (in  $\text{cm}^3$ ) are, respectively, the pressure of the upstream chamber and the volume of the downstream chamber,  $A$  (in  $\text{cm}^2$ ) and  $l$  (in cm) are, respectively, the area and thickness of the membrane, whereas  $S$  (in  $\text{cm}^3$  (STP)  $\text{cm}^{-3}$   $\text{cmHg}^{-1}$ ) and  $D$  (in  $\text{cm}^2 \text{s}^{-1}$ ) are, respectively, the solubility and diffusion coefficients. With these units,  $p(t)$  is obtained in cmHg.

In steady-state conditions ( $t \rightarrow \infty$ ), Eq. (1) becomes a

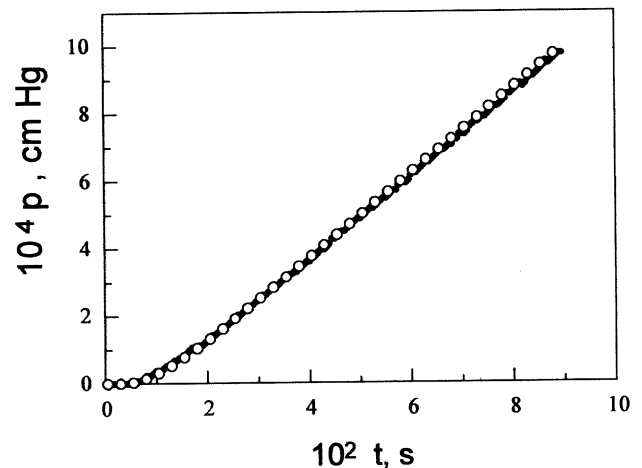


Fig. 2. Variation of the pressure of helium in the downstream chamber with time at  $30^{\circ}\text{C}$ . Experimental results (continuous line). Values calculated by means of Eq. (1) (○).

straight line given by

$$p(t) = 0.2876 \frac{p_0 A l S T}{V} \left( \frac{Dt}{l^2} - \frac{1}{6} \right) \quad (2)$$

that intercepts the time axis at  $\theta = l^2/6D$ , where  $\theta$  is the time lag. Hence [7],  $D = l^2/6\theta$ .

Since the permeability coefficient is  $P = DS$ , this parameter is given by

$$P = 3.590 \frac{Vl}{p_0 A T} m \quad (3)$$

where  $m$  is the slope of the straight line  $p(t)$  versus  $t$  in the steady-state regime. In this expression,  $P$  is obtained in barrers [ $1 \text{ barrer} = 10^{-10} (\text{cm}^3 (\text{STP}) \text{cm cm}^{-2} \text{s}^{-1} \text{cmHg}^{-1})$ ].

The permeability results, shown in Fig. 3, indicate that the permeability coefficient of helium in the membranes is nearly independent on the pressure of the upstream

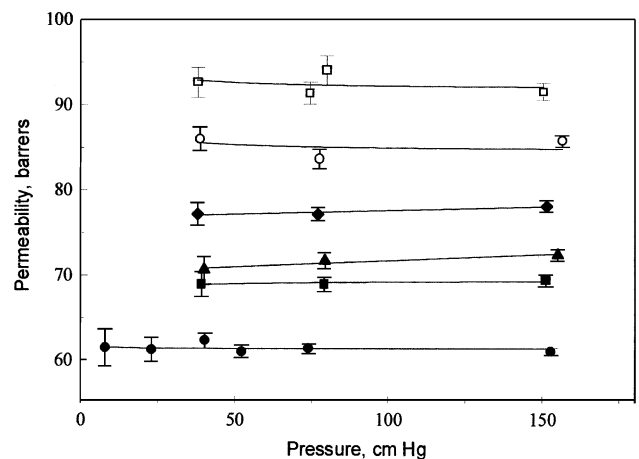


Fig. 3. Dependence of the permeability coefficient of helium on the pressure of the upstream chamber at different temperatures: (●)  $30^{\circ}\text{C}$ , (■)  $35^{\circ}\text{C}$ , (▲)  $40^{\circ}\text{C}$ , (◆)  $45^{\circ}\text{C}$ , (○)  $50^{\circ}\text{C}$  and (□)  $55^{\circ}\text{C}$ .

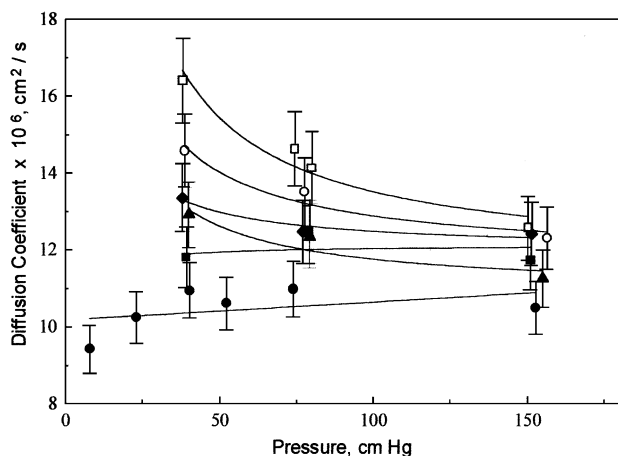


Fig. 4. Variation of the diffusion coefficient of helium in the polycarbonate membrane at different temperatures: (●) 30°C, (■) 35°C, (▲) 40°C, (◆) 45°C, (○) 50°C and (□) 55°C.

chamber. The values of the diffusion coefficient at temperatures above 30°C, shown as a function of  $p_0$  in Fig. 4, seem to slightly increase as the pressure of the upstream chamber decreases. However, the relatively large uncertainty of the values estimated for the diffusion coefficient preclude the possibility of attributing any physical meaning to the pressure dependence observed for this quantity.

The permeability and diffusion coefficients obey to the Arrhenius relations

$$P = P_0 \exp\left(-\frac{E_P}{RT}\right) \quad (4)$$

$$D = D_0 \exp\left(-\frac{E_D}{RT}\right)$$

where  $E_P$  and  $E_D$  are, respectively, the activation energies of the permeability and diffusion coefficients. Two illustrative Arrhenius plots shown in Fig. 5 indicate that the values of  $E_P$  and  $E_D$  are 3.0 and 1.9 kcal mol<sup>-1</sup>, respectively. This means

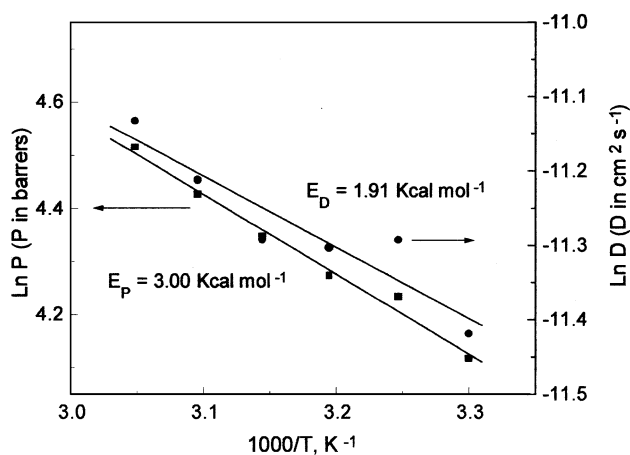


Fig. 5. Arrhenius plots for the permeability and diffusion coefficients of helium in the membrane.

that the heat of sorption is ca. 1.1 kcal mol<sup>-1</sup>, so the solubility of helium in the membranes is rather poor.

#### 4. Molecular simulations

Atomistic structures of glassy PBCDC were produced as explained elsewhere [5]. In brief, four polymer chains such as those shown in Fig. 1, each one of them containing  $x = 10$  repeat units (i.e. 3288 atoms in total) were packed into a cubic cell with side length of 33.98 Å subject to periodic boundary conditions (PBC). The Amber force field [8–11] was used to compute potential energies, and the Coulombic contribution to the potential was calculated as the sum of interactions between partial charges assigned to every atom by means of the MOPAC package [12] and the AM1 procedure employing a distance dependent effective dielectric constant. Cutoff distances of 9.6 and 8 Å were used, respectively, for Coulombic and van der Waals interactions.

In the TSA, the thermal fluctuations  $\delta$  of the positions of all polymer atoms are described by an isotropic Gaussian functional form with the same mean-square deviation  $\Delta^2$  for all of them, given by

$$W(\delta) \propto \exp\left(-\frac{\delta^2}{\Delta^2}\right) \quad (5)$$

The parameter  $\Delta$  is customarily referred to as smearing factor and accounts for the difference between thermal linear motion of the diffusant particle and fast mobility of the atoms in the polymeric host matrix due to bond lengths vibration and bond angle bending. An exact determination of this parameter becomes virtually impossible. However, rough estimations [13,14] assuming that each atom of the matrix has an overall energy equivalent to the thermal value  $3kT/2$ , is linked to some neighbors by chemical bonds having typical bonds lengths of ca. 1.5 Å and stretching force constants of ca. 600 kcal mol<sup>-1</sup> Å<sup>-2</sup> and bond angles with bending force constants of ca. 0.01 kcal mol<sup>-1</sup> deg<sup>-1</sup> suggest values of ca. 0.3–0.4 Å for the thermal oscillation represented by  $\Delta$ . In the present work, we shall use a value of  $\Delta = 0.3$  Å which has been employed for many other systems [5,13–16] producing good agreement between experimental and calculated values of the diffusion coefficient. Despite using a fixed value of  $\Delta = 0.3$  Å for the computation of values that are compared with experimental results, some calculations were also performed with different values of  $\Delta$  in order to explore the effect of this parameter in the calculated magnitudes.

An orthogonal equispaced net of 10<sup>6</sup> positions with intervals of  $d = 0.34$  Å was used, and the interaction energy between the host polymer atoms and the guest diffusant at the grid points was calculated in the pair approximation. The limits of site  $i$  were obtained by choosing the steepest descent gradient from every point of the grid which will terminate in one of the local potential energy minimum. The partition function of each site depends on both its

depth and extent, i.e. the value of the energy at the bottom and the number of grid points that belongs to it. This partition function determines the mean residence time for the guest atom in the site.

In some cases, the crest surface separating two adjacent sites may be too small as to allow the passage of the diffusant, i.e. the diameter of the passage between sites  $i$  and  $j$  may be smaller than the cross-sectional area of the particle that is supposed to pass through it. It is then convenient to weight the rate constant of the diffusant transition from site  $i$  to adjacent site  $j$  with a factor given by [5]

$$w_{ij} = \frac{\delta_{ij}}{S_D} \quad (6)$$

where  $S_D$  is the cross-sectional area of the diffusing particle and  $\delta_{ij}$  is zero when the crest surface is smaller than  $S_D$  and the unit otherwise.

The trajectory of the diffusant in the matrix is simulated by a random walk of the particle in the grid. The walk consists of a series of jumps from a one initial site to a neighbor one. It is assumed that the time required for each jump is equal to the mean residence time of the site from which the jump takes place. The rate of the diffusant transition from site  $i$  to site  $j$  is given by [4]

$$R_{ij} = w_{ij} \left( \frac{kT}{8\pi m} \right)^{1/2} \frac{Z_{ij}}{Z_i} \quad (7)$$

where  $kT$  is the thermal energy,  $m$  the mass of the diffusant,  $Z_{ij}$  the configuration partition function at the crest surface separating the states  $i$  and  $j$ , whereas  $Z_i$  is the partition function for the valley of site  $i$ . The probability for the  $ij$  transition is

$$p_{ij} = \tau_i R_{ij} \quad (8)$$

where  $\tau_i$  is the mean residence time for the guest atom in site  $i$  given by

$$\tau_i = \frac{1}{\sum_k R_{ik}} \quad (9)$$

where the sum expands over all the sites adjacent to  $i$ .

According to the TSA, the solubility coefficient can be written as

$$S = \frac{1}{kTV} \int_V \exp\left(-\frac{E}{RT}\right) dV = \frac{1}{kT} \frac{Z}{N} \quad (10)$$

where  $V$  is the volume of the polymer matrix and  $N$  is the number of grid points employed to compute the partition function.

## 5. Computational results

Fig. 6 depicts the computed time dependence of the mean-square displacement of helium in the polycarbonate matrix for different values of the smearing factor  $\Delta$ . For

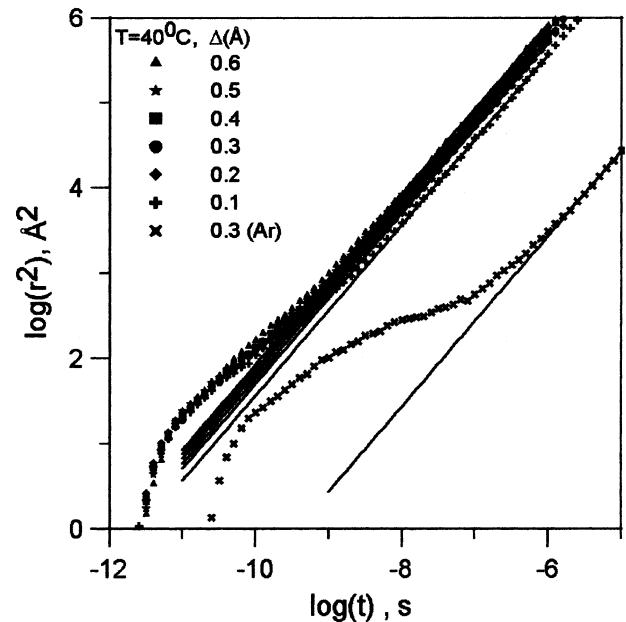


Fig. 6. Computed dynamics of helium in the polycarbonate membrane, at 40°C, for different values of the smearing factor. The curve corresponding to argon for  $\Delta = 0.3 \text{ \AA}$  is also shown.

comparative purposes, the variation of  $\langle r^2 \rangle$  with time for argon using  $\Delta = 0.3 \text{ \AA}$  is also shown. The dynamics behavior becomes diffusive at long times, thus allowing the calculation of the diffusion coefficient by means of the so-called Einstein relationship [4,8]

$$D = \frac{1}{6} \lim_{t \rightarrow \infty} \left\{ \frac{\partial}{\partial t} \langle (\mathbf{r}(t) - \mathbf{r}(0))^2 \rangle \right\} \quad (11)$$

where  $\mathbf{r}$  is the vector position of the diffusing particle in the matrix. The diffusion coefficient is strongly dependent on the smearing factor as can be seen in Fig. 7 where  $D$  is

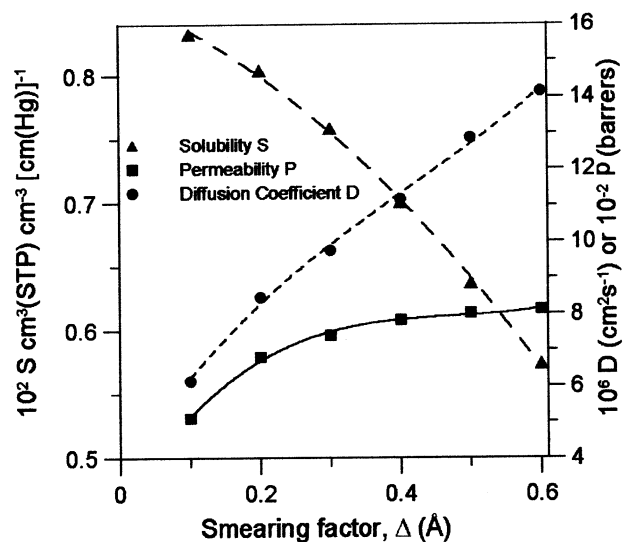


Fig. 7. Values of the diffusion and solubility coefficients as a function of the smearing factor  $\Delta$ .

plotted as a function of  $\Delta$ . The value of  $D$  computed for helium at 40°C for  $\Delta = 0.3 \text{ \AA}$  is  $9.8 \times 10^{-6} \text{ cm}^2 \text{ s}^{-1}$ , in rather good agreement with the experimental result,  $1.2 \times 10^{-5} \text{ cm}^2 \text{ s}^{-1}$  at the same temperature. The dynamics of helium is very fast when compared with that of argon. As can be seen in Fig. 6, in the region between the initial steps and the diffusive regime the relation  $\langle r^2 \rangle \propto t^n$  holds with  $n < 1$ . However, the diffusive regime for helium is reached at times that are two orders of magnitude lower than for argon. Without using the restriction introduced by Eq. (6) in the diffusion dynamics, the values of  $D$  obtained for helium and argon in the membranes used in this work amount to  $6.4 \times 10^{-5}$  and  $7.8 \times 10^{-7} \text{ cm}^2 \text{ s}^{-1}$ , respectively, which are significantly higher than the experimental results,  $1.2 \times 10^{-5}$  and  $4.5 \times 10^{-8} \text{ cm}^2 \text{ s}^{-1}$ , respectively [5].

The values computed for the diffusion coefficient of helium exhibit a rather weak temperature dependence. In the temperature interval 30–55°C, the calculated values of  $D$  only increase from  $9.4 \times 10^{-6}$  to  $9.7 \times 10^{-6} \text{ cm}^2 \text{ s}^{-1}$ , whereas the experimental values in the same interval change from  $9.4 \times 10^{-6}$  to  $1.6 \times 10^{-5} \text{ cm}^2 \text{ s}^{-1}$ . In principle, the computed values of the diffusion coefficient depend on temperature, density of the host matrix ( $\rho$ ) and the smearing factor ( $\Delta$ ). Therefore, the activation energy of the diffusion coefficient can be expressed by [17]

$$E_D = -\frac{dD}{d(1/T)} = -\frac{\partial D}{\partial(1/T)} - \frac{\partial D}{\partial \rho} \frac{\partial \rho}{\partial(1/T)} - \frac{\partial D}{\partial \Delta} \frac{\partial \Delta}{\partial(1/T)} \quad (12)$$

It has been found that for most diffusants the smearing factor accounts for more than 50% of  $E_D$ , but surprisingly the density contribution is rather small compared to the other two factors. The analysis of the diffusion argon in PBCDC membranes [5] indicates that the experimental variation of  $D$  with temperature may be reproduced by assuming that  $\Delta$  increases with  $T$  at the rate of  $0.005 \text{ \AA K}^{-1}$ . Since  $\Delta$  represents a balance among thermal motions, it seems reasonable to presume that it may change with  $T$ , but this is just a conjecture because an exact evaluation of the value of  $\Delta$  is precluded at this moment. At any rate, the diffusion coefficient of helium is not so sensitive to the variation of the smearing factor presumably as a consequence of the small size of the atoms of this gas.

Values of the solubility coefficient of helium in the membranes are plotted as a function of the smearing factor in Fig. 7. It can be seen that  $S$  decreases from  $8.3 \times 10^{-3} \text{ cm}^3$  (STP)  $\text{cm}^{-3} \text{ cmHg}^{-1}$  for  $\Delta = 0.1 \text{ \AA}$  to  $5.7 \times 10^{-3}$ , in the same units, for  $\Delta = 0.6 \text{ \AA}$ . These results, however, are nearly one order of magnitude higher than the experimental value of the solubility coefficient. Since the typical accuracy of the force fields at evaluating the free energies of molecules may not be better than four times the thermal energy ( $4kT$ ) per atom [18], the solubility coefficients of such light gases as helium surely cannot priory be estimated to better than one order of magnitude. It should be pointed out,

however, that good agreement between simulated and experimental values of the solubility coefficient was obtained for argon using the same force field employed here.

## 6. Conclusions

The transport of helium in PBCDC does not show a definite dependence on the pressure of the upstream chamber. This behavior suggests that adsorption processes that usually take place in glassy membranes are not detected in this study due to both the rather small upstream pressures employed and to the very small affinity diffusant-matrix.

The TSA gives a good account of the dynamics of helium in the polymer matrix provided that the transitions of the diffusant from site to adjacent sites is weighted by a factor that takes into account the ratio of the crest surface to the cross-sectional area of the atom of helium.

## Acknowledgements

This work was supported by the CAM and the DGESIC through the Grants DTM/0069/1998 and PB97-0778, respectively.

## References

- [1] Castello LM, Koros WJ. *J Polym Sci: Part B: Polym Phys* 1994;32:701.
- [2] McCaig MS, Seo ED, Paul DR. *Polymer* 1999;40:3367.
- [3] Gentile FT, Arizzi S, Suter UW, Ludovice PJ. *Ind Eng Chem Res* 1995;34:4193.
- [4] Gusev AA, Müller-Plathe F, van Gunsteren WF, Suter UW. *Adv Polym Sci* 1994;43:1977.
- [5] López-González M, Saiz E, Guzmán J, Riande E. *Macromolecules* 2001;34:000.
- [6] Crank J. *The mathematics of diffusion*. Oxford: Oxford University Press, 1975.
- [7] Barrer RM. *Trans Faraday Soc* 1939;35:628.
- [8] Weiner SJ, Kollman PA, Nguyen DT, Case DA, Singh UC, Ghio C, Alagona G, Profeta S, Weiner PJ. *J Am Chem Soc* 1984;106:765.
- [9] Weiner SJ, Kollman PA, Nguyen DT, Case DA. *J Comp Chem* 1986;7:230.
- [10] Homans SW. *Biochemistry* 1990;29:2110.
- [11] Cornell WD, Cieplak P, Bayly CL, Gould IR, Merz KM, Ferguson DMD, Spellmeyer C, Fox T, Caldwell JW, Kollman PA. *J Am Chem Soc* 1995;117:5179.
- [12] MOPAC, Quantum Chemistry Program Exchange, Department of Chemistry, Indiana University, Bloomington, IN.
- [13] Laguna MF, Guzmán J, Riande E, Saiz E. *Macromolecules* 1998;31:7488.
- [14] Laguna MF, Guzmán J, Saiz E, Riande E. *J Chem Phys* 1999;110:3200.
- [15] López-González M, Saiz E, Guzmán J, Riande E, submitted for publication.
- [16] Laguna MF, Saiz E, Guzmán J, Riande E, submitted for publication.
- [17] Gusev AA, Suter UW, Moll DJ. *Macromolecules* 1995;28:2582.
- [18] Gusev AA, Suter UW. *J Chem Phys* 1993;99:2228.